Pulse Generator Monocycle Gaussian for UWB Applications

MOHAMED DHIEB, MONGI LAHIANI and HAMADI GHARIANI
Laboratory of Electronics and Technology of Information (LETI)
National Engineers school of Sfax
Electrical Engineering Department. B.P. W, Sfax, TUNISIA 3038
mohamed_dhieb@yahoo.fr mongi.lahiani@enis.rnu.tn hamadi.ghariani@enis.rnu.tn

Abstract: - This paper focuses on the study and design of a simple MOS generator circuit which provides the first derivative of the Gaussian pulse from input rectangular signal. To generate wavelets required in an ultra-wideband (UWB) impulse radio, the first derivative of the Gaussian function is approximated by combining four hyperbolic tangent functions (tanh). Afterwards, four differential pairs are used. The output generator circuit is ultra short monocycle pulses about 244 ps width alternately in phase and in opposition of phase. The generated width pulse can be adjusted by changing the rise and fall time of the input signal. Simulations show that a good approximation of this waveform is possible while using integrated coefficients. A MOS transistor circuit implementation is presented and its simulation results are shown. Comparisons between theoretical and simulation tests are detailed in order to validate the design and the good functioning of the complete structure. . Furthermore, the 2.5 V voltages supply, relative to the chosen MOS 0.35µm technologies (AMS foundry), allows the reduction of the system power consumption.

Key words— Transfer function, Hyperbolic tangent, MOS transistors differential pair, Monocycle pulses, Ring oscillator.

1 Introduction

Ultra Wide Band (UWB) is a wireless communication technology which is to transmit (telecommunications) or collect (radar) data using pulse signals of short duration and then would have a broad spectrum of frequencies. It has been strongly emphasized in recent years (particularly since 2002 [1]) and several areas of this type of communications are being considered.

The pulse generator circuit is one of the most sensitive in communication link Ultra Wide Band (UWB) [2].

There are several techniques and approaches for the generation of short pulses in the order of the nanosecond. A century ago, a conventional method of generation of ultra-short pulses was based on using electric arc generators [3]. With technology evolution, a range of components was used. Thus, we find pulse generators based on transistors operating in the avalanche mode, which require high voltages for polarization. But we also find generators based on Step Recovery Diodes (SRD) [4], on tunnel diodes or avalanche diodes [5] and the sinusoidal source [6].

The use of sinusoidal source to generate sinusoidal monocycle pulse is an excellent choice, but the delicate point is the synchronization of the whole circuit. It is based on the SRD diode leads to generation the Gaussian monocycle pulse. It is consisted of Schottky diode and stubs.

Recently, we have presented a review on the existing techniques to generate short pulses. Now we introduce a new generation Gaussian monocycle pulses for ultra wide band applications. This approach is relies on the exploitation of the property of the transfer function of a differential pair of transistors. Therefore, a monocycle pulse generator circuit based on a combination of differential pairs of MOS transistors is presented and detailed thereafter.

In this paper, we begin first with an overall architecture of transmitter ultra wide band. After, we describe the operating principle of a transmitter ultra wide band. Then, we show interests in detail of a few blocks of the transmitter. The first considered element is the ring oscillator whose basic architecture is formed by the association in series of an odd number of curly inverters and allowing generating a rectangular signal. The second proposed element is a new circuit generator Gaussian monocycle pulse based on four differential pairs of MOS transistors designed having AMS of 0.35µm technology. The various simulation results of this circuit in the time and frequency domain are presented.

2 General Architecture of the UWB Transmitter

We propose general architecture of ultra-wide band transmitter, which consisting of three blocks:

- Ring oscillator generating a rectangular signal frequency 400MHz.
- Pulse generator to generate monocycle pulse in the order of wide is 244 ps.
- Band pass filter [3.1 - 5.1 GHz] for formatting pulses under spectral mask defined by the FCC (Federal Communication Commission).U.S. (United States).

The proposed architecture is shown in figure 1:

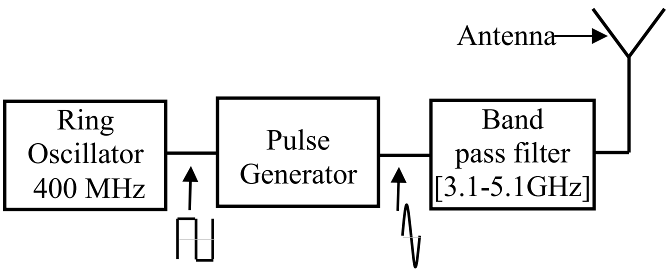

Fig.1 Proposed general architecture UWB transmitter

As illustrated in the schema above, from the ring oscillator, we obtain a rectangular signal frequency 400 MHz. The rectangular signal is obtained with an adjustable rise and full time. This in turn is applied to the pulse generator, which generates monocycles pulses alternative in phase and in opposition of phase. These impulses will be shaped by the band pass filter [3.1 - 5.1 GHz] in accordance with U.S. regulations of the FCC [1, 7].

3 Study and Design the Some Blocks of the UWB Transmitter

In this part, we are interested to design two blocks: the ring oscillator and impulse generator. First, the CMOS ring oscillator whose role is to generate a rectangular signal, and then we discuss the design of the generator circuit: main part of the Gaussian monocycle pulse. It represents the most important block of our transmitter chain. The temporal and spectral studies of the ultra wide band transmitter are made using the Advanced Design System (ADS).

3.1 Ring Oscillator

The ring oscillator in figure 2 is a circuit with an odd number of inverters in series interspersed by capacity and looped between themselves. The output of the last inverter commands the input of the first.

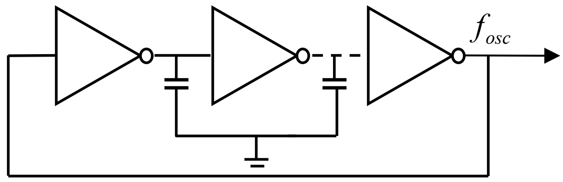

Fig.2 Ring oscillator principle

The number of inverters, the values of capacity and size of transistors allow us to adjust the oscillation frequency to the desired value. This frequency is given by the expression (4), which is deducted from the expressions (1), (2) and (3) [8].

$$f_{osc} = \frac{1}{N(tp_{HL} + tp_{LH})} \quad (1)$$

With: tp_{HL} and tp_{LH} is the delay times respectively to coming down and the rise of every inverter and N represents the number of inverters used.

$$tp_{HL} = \frac{4C}{K_P \frac{W_P}{L_P} V_{dd}} \quad (2)$$

$$tp_{LH} = \frac{4C}{K_N \frac{W_N}{L_N} V_{dd}} \quad (3)$$

With: K_P and K_N, represent the intrinsic transconductances of the PMOS and NMOS transistors, W_P and W_N represent transistors widths, L_P and L_N represent channels transistors lengths and C represents the value of the capacity used.

If we put: $\frac{W_P}{L_P} = 2\frac{W_N}{L_N}$ [8], the frequency oscillation expression becomes then:

$$f_{osc} = \frac{2K_N\left(\frac{W_N}{L_N}\right)V_{dd}}{19.2NC} \quad (4)$$

With: K_N =2.8 K_P [8].

To validate the operation of circuit pulse generator, we propose a circuit of CMOS ring oscillator in figure 3. This circuit is composed of five inverters in series interspersed by capacity and looped between each structure. The output is a rectangular signal with amplitude of 5V and a frequency of 400MHz.

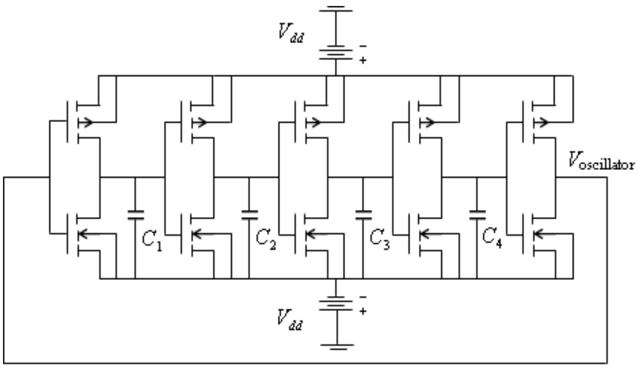

Fig.3 CMOS ring oscillator circuit

According to equation (4), we deduce the value of the capacity: C = 0.058 pF, avec K_N = 77.498 10^{-6}, W_N = 1μm and W_P = 2μm.

The rectangular curve in figure 4 is the output signal of CMOS ring oscillator circuit. Thus, we obtain a rectangular signal that will be applied thereafter to the monocycle pulse generator.

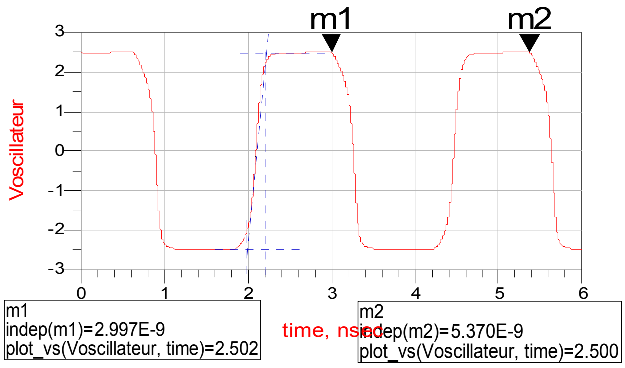

Fig.4 Output signal rectangular of a CMOS ring oscillator

According to figure 4, the period of the rectangular signal ring oscillator is T_{osc} = 2.373 ns, therefore the signal frequency is f_{osc} = 421 MHz, which join the theoretically calculated frequency and the practice rise time t_m = 0.21 ns corresponds to that theoretically calculated $t_m = tp_{LH}$ = 0.209 ns.

3.2 Monocycle Pulse Generator

The pulse generator which we propose is a generator that delivers very short monocycle pulses of the order 244 ps. These pulses will be used in the ultra wide band system block transmitter. The standard of generation is to represent the monocycle pulse as a mathematical function consisting of a sum in terms of hyperbolic tangent. These will be achieved through the property in the transfer function of the transistors differential pair [9]. We now analyze the theory, based on two approaches demonstrate the approximation between the hyperbolic tangent and the transfer function of the MOS differential pair [10]. The transfer functions presented in [10] are nonlinear functions; they are used to obtain signals with specific forms. For example, conversion of a triangular signal into a sinusoidal signal is the best known of the transfer function of the bipolar transistors differential pair [11]. This transfer function was also used by J. F. M. Gerrits and J. R. Farserotu [12] to propose a mathematical function representing the momentum of the second derivative of Gaussians used in some ultra wide band systems receiving pulse. For us, we propose another function mathematical generating the Gaussian monocycle pulse, and thereafter, a circuit to generate a mathematical function, but this time using MOS transistors differential pairs.

3.2.1 Mathematical Function of the Monocycle Pulse

The design a generation circuit of Gaussian monocycle pulse is composed just of the integrated components (transistors, capacitors and inductors). And knowing that the terms in hyperbolic tangents can be obtained easily by structures transistors differential pairs as we showed in the article [10], we tried to model the momentum monocycle pulse by a mathematical function that contains such terms. Thus, the mathematical function that we propose is as follows [10]:

$$A(x) = -\tanh(x+2) + \tanh(x+5) + \tanh(x-2) - \tanh(x+1) \quad (5)$$

It is an expression composed of four terms in hyperbolic tangent. As we showed in the article [10], the function A (x) is a very good approximation of the Gaussian monocycle pulse.

The circuit which achieves the function *A (x)* is a transistor differential pair. The function *A (x)* is composed of four terms in hyperbolic tangent. What we distinguish is the fact that these terms are shifting the one to the others. This shift of the position of zero amplitude is indicated thereafter. The generator circuit is constituted of four transistors differential pairs, so that each differential pair generates a term hyperbolic tangent.

In what follows, we present the circuit to achieve the function *A (x)* in order to generate monocycle pulse.

3.2.2 Design of the monocycle pulse generator

Here, we first explain the design of different parts that constitute the global circuit of the monocycle pulse generator. This architecture of the Gaussian monocycle pulse generator is based on four NMOS transistors differential pairs placed in parallel and fed by a rectangular voltage that is generated by the CMOS ring oscillator.

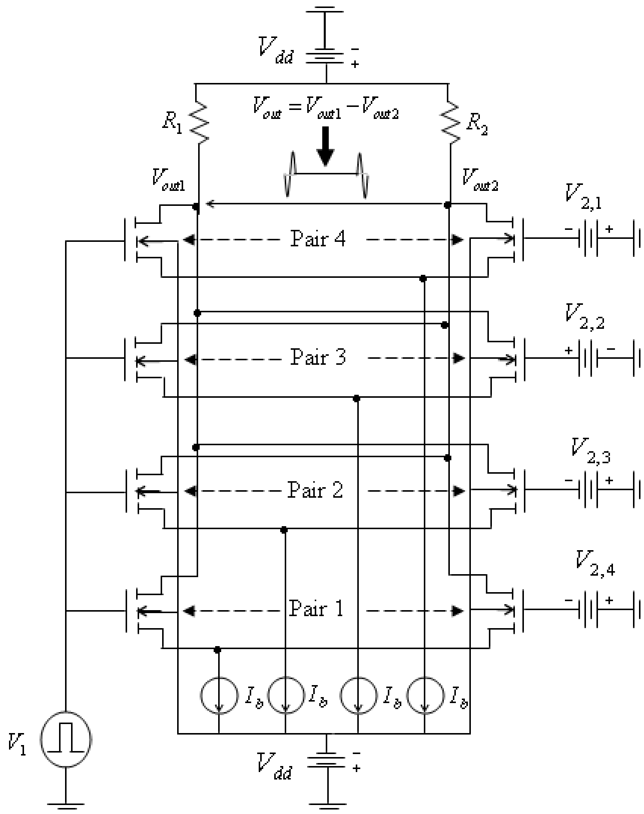

Fig.5 Monocycle pulse generator circuit

If a rectangular signal is applied to the input of the generator circuit, we obtain a sequence of monocycle pulse out. The circuit function of figure 5 simply allows making the mathematical function *A (x)*. The two negative terms of this function (-tanh(x+2) and -tanh(x+1)) are obtained by crossing two outings differential pairs that generate them with the other two differential pairs with positive terms. These are the second and third differential pair. The current sources, placed on common sources of transistors constituting the differential pairs, are there to control the amplitude of the generate term, approaching a hyperbolic tangent. Since they have the same magnitude, we connect the same current sources on the four differential pairs. The time shift function is ensured by the bias voltage applied to the four gates on the right side of the circuit. These voltages control the position of the amplitude zero in terms of hyperbolic tangent.

The input signal (rectangular signal) and the drains bias voltage of four differential pairs are chosen according to the characteristics (amplitude and temporal width) of desired Gaussian monocycles pulses.

3.2.3 Offset Voltage of a Transfer Curve of Differential Pair

The Gaussian monocycle pulse is approximated to the sum of four terms in hyperbolic tangent, as we have previously expressed in the equation (5), whose each one is obtained from the voltage transfer curve of a NMOS transistors differential pair.

Adding tension V_{Offset} to tension V_{2i} in figure 5 is responsible for the shift in the transfer curve in tension compared to that obtained for $V_{Offset} = 0$.

The different offset tensions corresponding to each NMOS transistors differential pair are shown in figure 6.

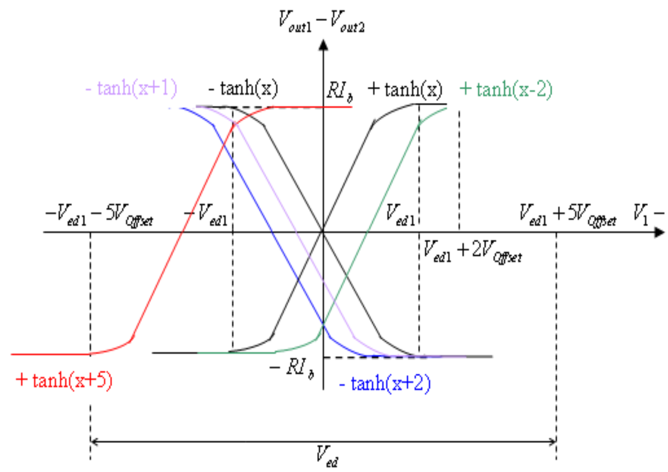

Fig.6 Offset voltage for each hyperbolic tangent

With:
V_{ed} : Interval of differential input voltage.
V_{Offset}: Offset voltage that corresponds to -tanh(x+1).

The interval of differential input voltage is expressed by the following equation:

$$V_{ed} = V_{ed1} + 5V_{\text{Offset}} - (-V_{ed1} - 5V_{\text{Offset}}) = 2V_{ed1} + 10V_{\text{Offset}} \quad (6)$$

Then:

$$V_{\text{Offset}} = \frac{V_{ed} - 2V_{ed1}}{10} \quad (7)$$

To ensure the intersection of the curve +tanh(x+5) with the curve -tanh(x+2) in figure 6, the offset voltage V_{Offset} must verify the following condition:

$$-V_{ed1} - 2V_{\text{Offset}} < V_{ed1} - 5V_{\text{Offset}} \Rightarrow V_{\text{Offset}} < \frac{2}{3}V_{ed1} \quad (8)$$

Different values of the components that constitute the NMOS transistor differential pair are grouped in table 1.

Table 1: Specifications and requirements of the differential pair

Parameters	Devices	Value
Resistance	R	200 Ω
Bias current	I_b	2.4 mA
Limit the zone of linear operation	V_{ed1}	1.04 V
Interval of differential input voltage	V_{ed}	5 V
Supply voltage	V_{dd}	2.5 V

According to equation (7) and using the values in table 1, the offset voltage that corresponds to -tanh(x+1) is V_{Offset} = 0.292 V.

The offset voltage and the two voltage limits of the linear operation zone V_{emin} and V_{emax}, which corresponds to each NMOS transistors differential pair, are given in table 2.

Table 2: Offset tensions and voltage limits of the linear operation zone values of each NMOS transistor differential pair

	V_{Offset} (V)		V_{emin} (V)		V_{emax} (V)	
hyperbolic tangent	Expression	value	Expression	value	Expression	value
-tanh(x+1)	$-V_{Offset}$	-0.292	$-V_{ed1}-V_{Offset}$	-1.332	$V_{ed1}-V_{Offset}$	0.748
+tanh(x-2)	$+2V_{Offset}$	+0.584	$-V_{ed1}+2V_{Offset}$	-0.456	$V_{ed1}+2V_{Offset}$	1.624
+tanh(x+5)	$-5V_{Offset}$	-1.46	$-V_{ed1}-5V_{Offset}$	-2.5	$V_{ed1}-5V_{Offset}$	-0.420
-tanh(x+2)	$-2V_{Offset}$	-0.584	$-V_{ed1}-2V_{Offset}$	-1.624	$V_{ed1}-2V_{Offset}$	0.456

The maximum value of the voltage transfer curve is given by $V_{o\ max}$ = RI_b = 0.480 V, thus for the minimum value which is given by $V_{o\ min}$ = -RI_b = -0.480 V.

The report $\frac{W}{L}$ of the NMOS transistors of differential pairs is determined as follows:

$$\frac{W}{L} = \frac{2I_b}{{V_{ed1}}^2 K_N} \qquad (9)$$

With: $K_N = \mu_n C_{ox}$ where μ_n is the mobility of electrons in the channel and C_{ox} is the grid capacity per unit area.

We determine in the first, the value K_N then to deduce the width of the transistor channel W.

While basing itself on the study made in the article [10], we find then:

$$\mu_n C_{ox} = \frac{2LI_d}{W\left(V_{GS}-V_{TH}\right)^2} = 77.498\ \ 10^{-6},$$

with $V_{TH} = 4.979.10^{-1}$, then $\frac{W}{L} = 57.264$.

If one takes $L = 0.35\ \mu m$, then the width of the channel transistor $W = 20\mu m$.

We use the NMOS transistor of foundry AMS 0.35µm in saturation region with the precedent conditions to verify the operating point that we have chosen.

We find that the circuit is polarized by a voltage V_{GS} = 1.54 V on the grid and V_{DS} = 2.5 V on the drain. We recall that the purpose of choosing a polarization point in the saturation regime is to provoke approximation of the voltage transfer curve of the NMOS transistors differential pair with the term hyperbolic tangent shown in [10].

3.2.4 Voltage Transfer Curves of NMOS Transistor Differential Pair

The voltage transfer curves of NMOS transistor differential pair, which corresponds to -tanh(x+1), +tanh(x-2), +tanh(x+5) and -tanh(x+2) are represented in figure 7.

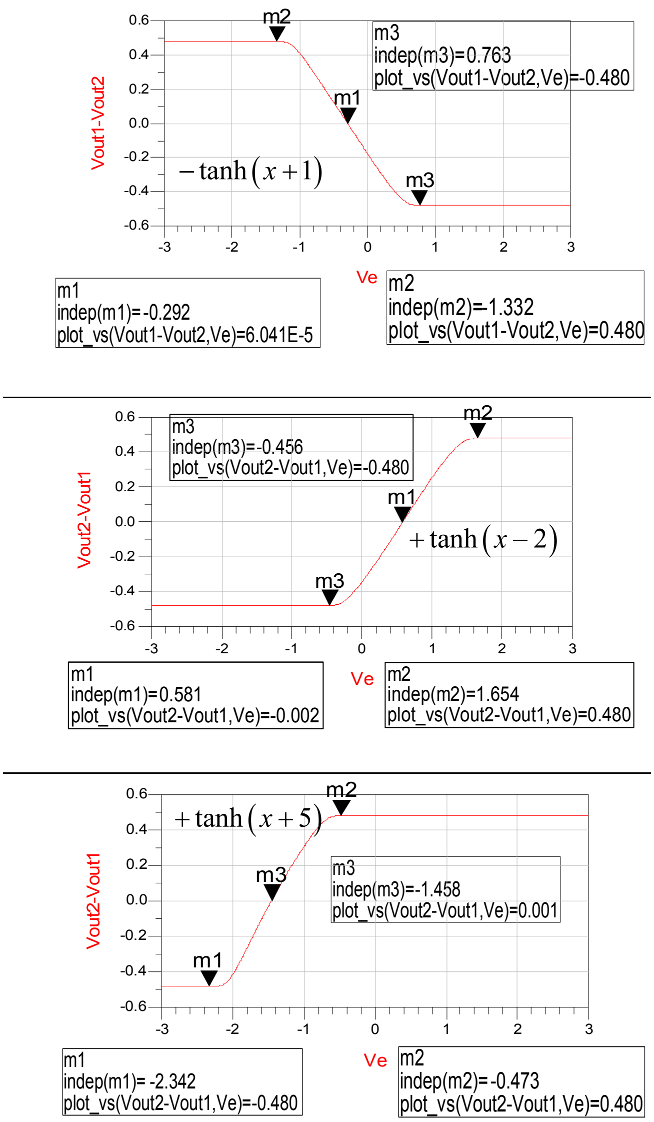

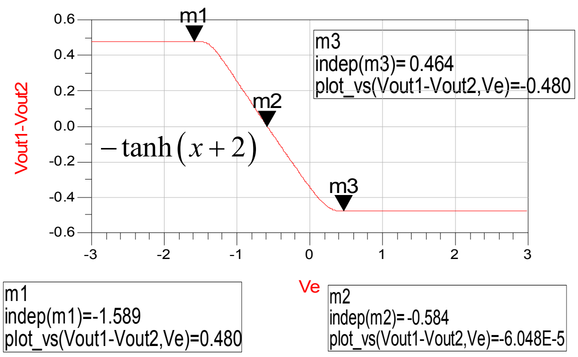

Fig.7 The voltage transfer curves, which corresponds to-tanh(x+1), +tanh(x-2), +tanh(x+5) and -tanh(x+2)

Referring to the curves of figure 7, the voltage limits V_{emin} and V_{emax} are determined. The maximum and minimum value of each voltage transfer curve and offset voltage V_{Offset}, correspond to those theoretically calculated.

The four voltage transfer curves and their sum are shown in figure 8.

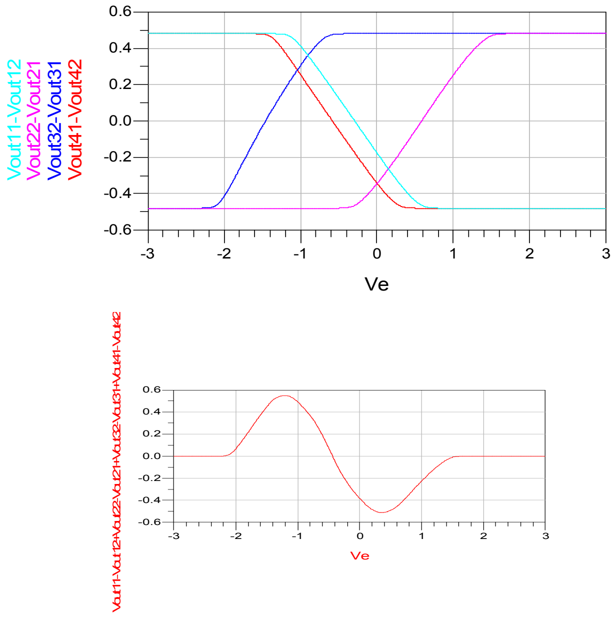

Fig.8 Sum of the four voltage transfer curves

We note from figure 8, the sum of four voltage transfer curves, which correspond to -tanh(x+1), +tanh(x-2), +tanh(x+5) and -tanh(x+2) are approximated to a Gaussian monocycle pulse.

3.2.5 Temporal Study of NMOS Transistors Differential Pairs

The temporal study of a NMOS transistors differential pair is obtained by applying to the input a rectangular voltage of 5V amplitude and 400MHz frequency.

The temporal response of four differential pairs of the figure 9 corresponding to -tanh(x+1), +tanh(x-2), +tanh(x+5) and -tanh(x+2) are obtained by choosing the voltage $V_2 = V_{Offset}$ of table 2.

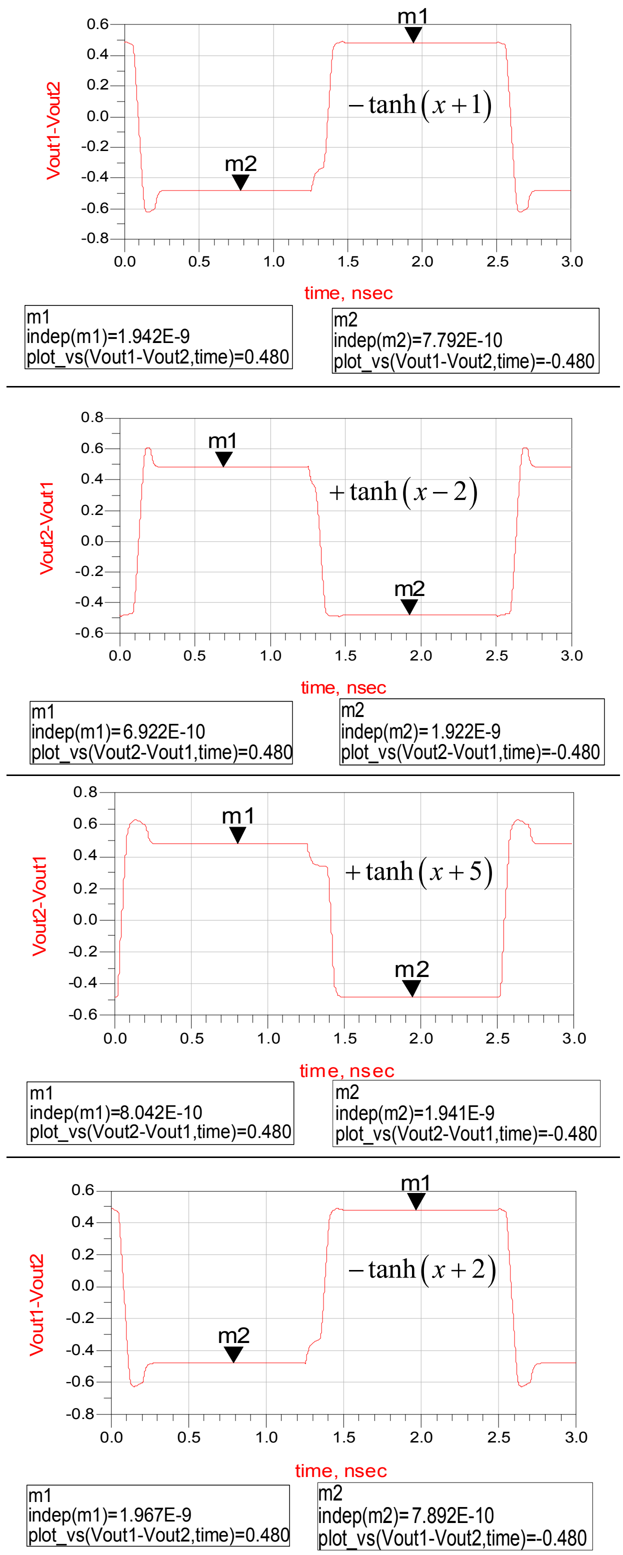

Fig.9 Temporal response of four differential pairs

According to the curves of figure 9, we note that the temporal response of four NMOS transistors differential pairs saturate the values theoretically calculated $V_{o\ min}$ = -0.480 V and $V_{o\ max}$ = 0.480 V.

3.2.6 Simulations of the Monocycle Pulse Generator

The monocycle pulse generator in figure 5 is formed by the parallel association of four NMOS transistors differential pairs that are already studied and it is powered to its input by a rectangular voltage generator of frequency 400 MHz which represents the repetition frequency of the series of Gaussian monocycle pulse. Thus, the curves below show the simulation results obtained with the circuit of figure 5 using the software ADS (Advanced Design System). These results are obtained by using the transistor model AMS 0.35µm and the ideal components of the library ADS for the rectangular signal source and current sources.

➢ Temporal study

The temporal study of the monocycle pulse generator allows us to describe the characteristics of the pulses generated in amplitude and frequency terms.

After simulations on the optimization of various parameters of the polarization circuit, we took current sources of 2.4mA, a drains biasing of 2.5V and a rectangular source with amplitude about 5V peak to peak and rise time of the order 200 ps.

The monocycle pulse generator creates at its output a series of Gaussian monocycle pulse with frequency of 400 MHz, the results are mentioned in figure 10.

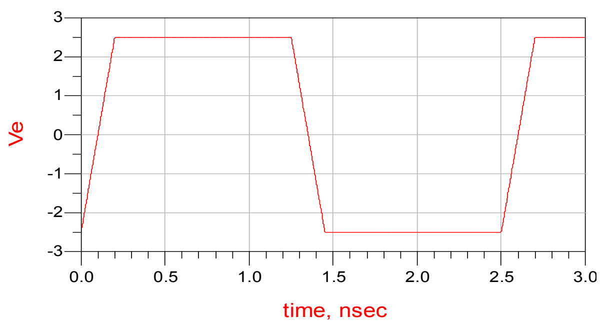

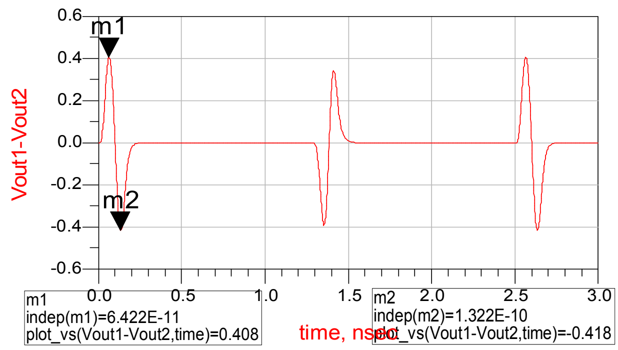

Fig.10 Simulations results of circuit monocycle pulse generator

The first curve in figure 10 represents the rectangular signal applied to the input circuit and the second curve represents the sequence of monocycles pulses generated. We note that pulses are triggered at each rising or falling front. We also note that monocycles pulses generated with rising fronts begin with the positive semi-cycle (what we call the pulse in phase). In contrast the monocycles pulses generated with falling fronts begin with the negative semi-cycle (what we call the pulse in opposition of phase). We then deduce that the sequence of pulses generated is consisted of the succession of pulses in phase and opposition of phase. However, these pulses have the same temporal width and almost the same magnitude as shown in figure 10.

A single Gaussian monocycle pulse is shown in figure 11:

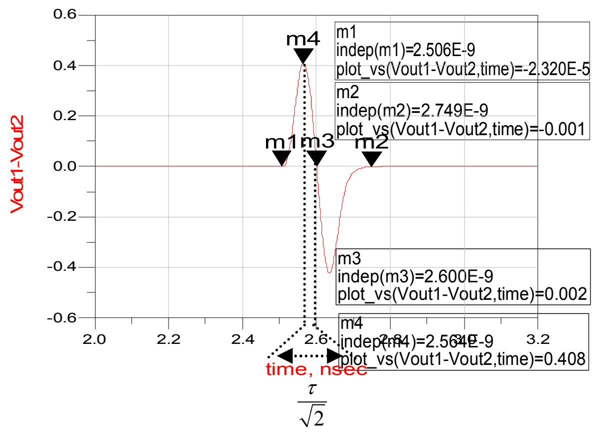

Fig.11 A single Gaussian monocycle pulse

According to figure 11, the period of the Gaussian monocycle pulse is $T_m = 0.243ns$, therefore the monocycle frequency is $f_{monocycle} = \frac{1}{T_m} = 4.115GHz$ corresponds to the theoretical frequency which is about $4.1GHz$.

The curve in figure 11 reached its maximum for $t = \frac{\tau}{\sqrt{2}} = 0.036ns$ [13], so the constant that allows to adjust the pulse width is $\tau = 0.0509ns$. The center frequency of the Gaussian monocycle pulse is $f_{c,monocycle} = \frac{1}{\pi\tau\sqrt{2}} = 4.421GHz$ [13].

- frequency study

The frequency study of the Gaussian monocycle pulse generator allows us to describe the characteristics of the pulses generated in terms of frequency band used and value of center frequency.

The Spectrum of a Gaussian monocycle pulse is shown in figure 12.

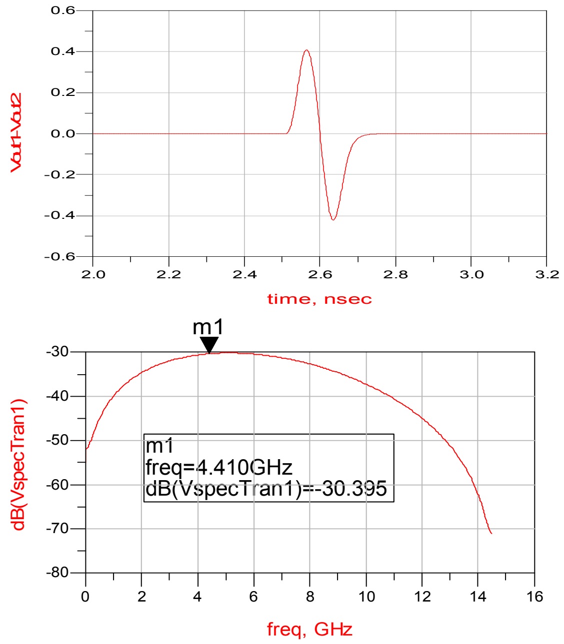

Fig.12 Spectrum of a Gaussian monocycle pulse

According to figure 12, the center frequency is $f_{c,monocycle} = 4.410GHz$ which corresponds to that obtained in the temporal study.

The Spectrum of a series of Gaussian monocycle pulses is shown in figure 13.

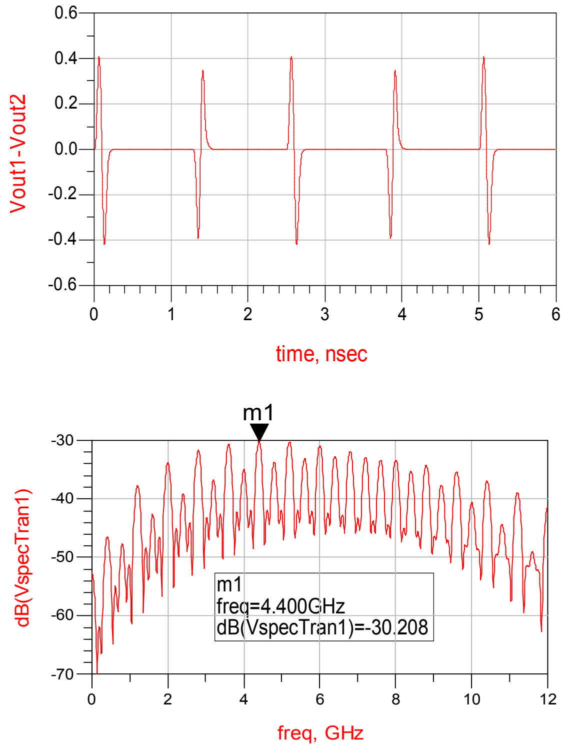

Fig.13 Spectrum of a series of Gaussian monocycle pulses

According to figure 13, the center frequency is $f_{c,monocycle} = 4.400GHz$ which corresponds to that obtained in the temporal study.

The frequency baseband of the Gaussian monocycle pulse must be selective to the band [3.1 - 5.1] GHz to respect the regulation constraints of the FCC.

4 Monocycle Pulse Generator Associated with a CMOS Ring Oscillator

The combination of a CMOS ring oscillator have the function of generation the rectangular signal, with a monocycle pulse generator represents the most important block of ultra wide band transceiver. This combination requires the addition of an adaptation circuit formed by a CMOS inverter represented in figure 14.

With $V_{2,1}$ = -0.292V, $V_{2,2}$ = 0.584V, $V_{2,3}$ = -1.46V, $V_{2,4}$ = -0.584V.

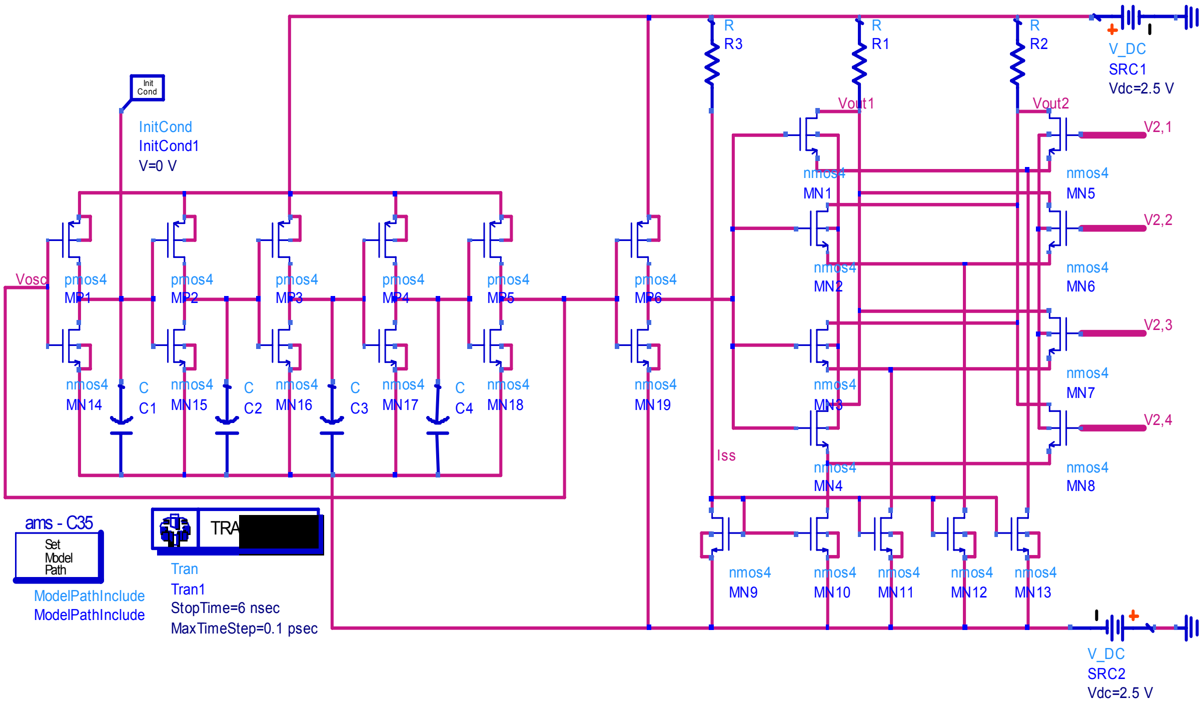

Fig.14 Monocycle pulse generator with a CMOS ring oscillator

The series of Gaussian monocycle pulses is shown in figure 15.

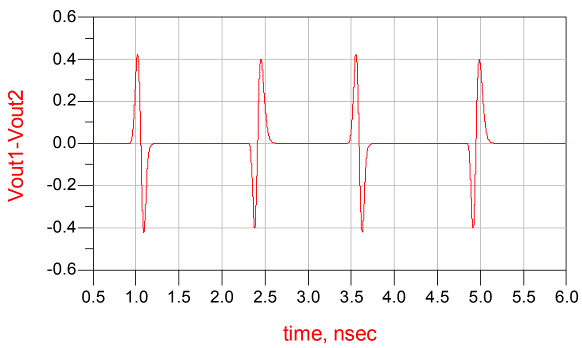

Fig.15 Series of Gaussian monocycle pulses

In figure 15 the generated Gaussian monocycle pulses are successively in phase and opposition of phase according to the transitions from the high and low levels of the rectangular signal and have amplitude of about 408 mV.

The comparison between theoretical and simulation results is given in Table 3.

Table 3: Comparison between theoretical and simulations performance characteristics of the monocycle pulse generator

Voltage (V) / Hyperbolic tangent	$V_{e\,min}$	$V_{e\,max}$	$V_{o\,min}$	$V_{o\,max}$	V_{Offset}	
$-\tanh(x+1)$	-1.332	0.748	-0.480	0.480	-0.292	Theoretical results
$+\tanh(x-2)$	-0.456	1.624	-0.480	0.480	+0.584	
$+\tanh(x+5)$	-2.5	-0.420	-0.480	0.480	-1.46	
$-\tanh(x+2)$	-1.624	0.456	-0.480	0.480	-0.584	
$-\tanh(x+1)$	-1.332	0.763	-0.480	0.480	-0.292	Simulation results
$+\tanh(x-2)$	-0.456	1.654	-0.480	0.480	+0.581	
$+\tanh(x+5)$	-2.342	-0.473	-0.480	0.480	-1.458	
$-\tanh(x+2)$	-1.589	0.464	-0.480	0.480	-0.584	

5 Conclusion

So far we have studied the design of a new Gaussian monocycle pulse circuit, which presence is essential in a chain of communication ultra wide band. Equally, we have conducted a study of a CMOS ring oscillator whose role is to generate a rectangular signal characterized by its oscillation frequency and transition duration. Thus, we have studied and designed a monocycle pulses generator circuit in technology AMS 0.35μm. This circuit is based on exploitation of the transfer function of a MOS transistor differential pair, in total it contains four NMOS transistor differential pairs, and the important simulation results are presented. Finally, we have simulated the global architecture of monocycle pulse generator containing the designed generator circuit. The simulation results are satisfactory.

Future work: we will study and design a filter ultra wide band [3.1 - 5.1 GHz] whose role is to filter ultra short Gaussian monocycle pulses (244 ps) issued by the pulse generator circuit given in this article. It among a plan to join to the spectral mask defined by the American regulations.

References:

[1] FCC 02-48, *"First Report and Order: Revision of Part 15 of the Commission's Rules Regarding Ultra-Wideband Transmission Systems"*, Federal Communications Commission, Adopted February 14, 2002, Released 22 April, 2002.

[2] J. Mallek, M. Dhieb, M. Lahiani & H. Ghariani : *"Générateur d'impulsions monocycle gaussien d'un émetteur Ultra Large Bande"*, Huitièmes Journées Scientifiques des Jeunes Chercheurs en Génie Electrique et Informatique (GEI 2008), Sousse, Tunisie, 17-19 Mars 2008.

[3] T. W. Barrett : *"History of Ultra Wideband (UWB) Radar & Communications: Pioneers and Innovators"*, Progress in Electromagnetics Symposium 200, Cambridge, MA, July 2000.

[4] N. Deparis, A. Bendjabballah, A. Boe, M. Fryziel, C. Loyez, L. Clavier, N. Rolland, P. A. Rolland : *"Transposition of a Baseband UWB Signal at 60 GHz for High Data Rate Indoor WLAN"*, IEEE Microwave and Wireless Components Letters, Vol. 15,No. 10, October2005.

[5] Y. W. Yeap : *"Ultra Wideband Signal Generation"*, Microwave Journal, September 2005.

[6] A. Azzakour, M. Regis, F. Pourchet, G. Alquié : *"Intégration d'une Nouvelle Source Ultra Large Bande en Technologie SIGE"*, l4émes Journées Nationales Microondes JNM, Nantes 11-13 Mai 2005.

[7] *"Revision of Part 15 oh the Commission's Rule Regarding Ultra Wideband Transmission Systems"* , FCC 02-48, First Report and Order, Washington, DC, 22 April 2002, http : //hraunfoss.fcc.cjov/edocspublic/attachmatch/ FCC-02-48A1 . pdf.

[8] F. Naghmouchi, M. Ghorbel, A. Ben Hamida, et M. Samet : *"CMOS ask system modulation dedicated to cochlear prothesis "*, IEEE, 0-7803-8379-6/04/$20.000, 2004.

[9] P. R. Gray, P. J. Hurst, S. H. Lewis, R. G. Meyer : *"Analysis and design of analog integrated circuits"*, Fourth Edition, 2001.

[10] Mohamed DHIEB, Mongi LAHIANI & Hamadi GHARIANI : *"Mathematical approximation of the hyperbolic tangent"* Sixth International Multi-Conference on Systems, Signals & Devices, SSD'2009, 23-26 March 2009, DJERBA- Tunisia.

[11] R. G. Meyer, W. M. Sansen, S. Lui : *"The Differential Pair as a Triangle-Sine Wave Converter"*, IEEE J. Solid-State Circuits, Vol 11, pp. 418-420, 1976.

[12] J. F. M. Gerrits, J. R. Farserotu : *"Wavelet Generation Ciruit for UWB Impulse Radio Applicattions"*, Electronics Letters, 5th, Vol. 38, No. 25, December 2002.

[13] M. Terré : *"Communication en ultra large bande (UWB)"* ; Cours du Conservatoire National des Arts et Métiers, Ce document est extrait d'une analyse des technologies UWB réalisée dans le cadre d'un projet RNRT (projet ERABLE). Il a été rédigé par les équipes de Thalès Communication (Gennevilliers), du centre de recherche Mitsubishi (Rennes), de l'Institut Eurecom (Sophia Antipolis) et du CNAM (Paris), Séminaire CNFRS/URSI, 2001.

Authors profile:

Mohamed Dhieb was born in Sfax, Tunisia, on November 1978. He received the Electrical Engineering Degree from the National Engineering school of Sfax (ENIS)-Tunisia in 2004, the Electronic Master diploma from National Engineering school of Sfax (ENIS)-Tunisia, in 2005 and the Doctorate of Engineer in Electrical from National Engineering school of Sfax (ENIS)-Tunisia, in 2010.

Actually he is working toward the Ph.D. degree at Sfax University. In 2004, he joined the Team of Micro-Electronics and Medical Electronic, Laboratory of Electronics and Technology of Information (LETI), as a Research. His research interests are the techniques Radar for measurement without contact of the physiological parameters of the man.

Mongi Lahiani was born in Sfax, Tunisia, in 1957. He received the Electrical Engineering Degree from the University of Sciences and Techniques of Sfax-Tunisia in 1984 and the Doctorate of Engineer in Measurement and Instrumentation from University of Bordeaux1, France, in 1986.
Since 1988, he has been a Professor at Sfax University. He joined the Sfax National School of Engineering in 1990 and he is a Professor in the fields of analog electronics and microelectronics. His research interests are design of circuits in medical electronic and integration of microwave circuits of microstrips with screen-printed thick films technology.

Hamadi Ghariani was born in Sfax, Tunisia, on July 1956. He received the Electrical Engineering Degree from the "University of Sciences and Techniques of Sfax-Tunisia"in 1981, the "DEA" degree in 1981and his "Doctorate of engineer" in 1983 in "Measurement and Instrumentation" from the "University of Bordeaux France". He joined the National Engineering School of Sfax since 1984. Actually he is a Professor in the same School. His research activities have been devoted to several topics: Medical Electronic; Communication systems for Medical Telemetry, Measure and Instrumentation.